A TUTORIAL ON FILTER BANKS AND WAVELETS[1]

Truong Q. Nguyen

University of Wisconsin, ECE Department
1415 Johnson Dr., Madison, WI 53706
nguyen@ece.wisc.edu

Abstract

This tutorial reviews the theory, structure and design methods for M-channel perfect-reconstruction (PR) filter banks. Some of the filter banks being considered here are the two-channel orthogonal filter bank; biorthogonal linear-phase filter banks; M-channel cosine-modulated filter banks and M-channel linear-phase filter banks. The connection with wavelet transform will be elaborated on the case of discrete dyadic wavelets (based on two-channel filter bank). Design examples of several filter banks and their applications in ECG and image compressions will be presented.

I. Introduction

Multirate filter banks are the fundamental building blocks for subband decompositions and frequency-domain/time-domain multiplexing. Fig. 1 shows the M-channel maximally-decimated filter bank where $H_k(z)$ and $F_k(z)$ are the analysis and synthesis filters, respectively. The analysis bank channelizes the input signal into many subbands using parallel set of bandpass filters. Similarly, the synthesis bank reconstructs the subband signals using a set of parallel filters. The forms of these filters depend on the applications and the dimensionality of the problem. The essential informations are extracted from the subband signals in the processing block. Its form varies and depends on the applications. For example, in the audio/image compression system, the spectral content of the subband signals are coded depending on their energies whereas in a radar system, the subband signals might be used to null out a narrow-band interference adaptively.

In the ideal environment where there is no processing on the subband signals, the output has aliasing and distortions because of the decomposition (filtering and decimation) and reconstruction (interpolation and filtering) processes. Perfect-reconstruction (PR) filter banks are systems where there is no error at the output, i.e., the output is a time-delayed copy of the input. Systems with small amount of aliasing and distortion are called Near-Perfect-Reconstruction (NPR) filter banks.

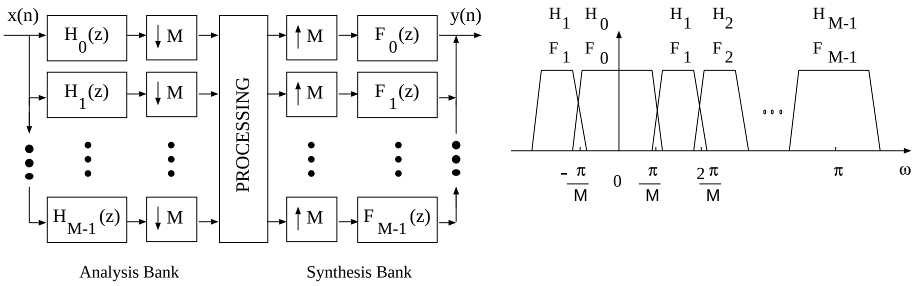

Figure 1: M-channel maximally-decimated filter bank.

The theory of two-channel orthogonal filter banks and the corresponding lattice structure are reported by Smith and Barnwell [1], Ramstad [2] and Vaidyanathan [3], respectively. The generalization to M-channel paraunitary filter bank is reported by Vetterli [4] and Vaidyanathan [5]. Two-channel orthogonal system cannot have linear-phase except in a simple structure (sum and difference of two delays). In order to obtain filter banks with linear-phase, orthogonal property must be sacrified which leads to the discovery of two-channel biorthogonal linear-phase filter banks [6, 8, 9, 10]. Linear-phase filter banks are used extensively in wavelet-based image coder and appeared in standard for fingerprint image compression [11].

[1]Will be presented at the International Conference on Digital Signal Processing, Cypress, June 95.

Efficient M-channel cosine-modulated filter banks are used in MPEG standard for audio compression [12]. These filter banks are first proposed by Nussbaumer [13] and Rothweiler [14] in the early 80's under the name of pseudo-QMF. These are not PR. The amount of aliasing is comparable to the stopband attenuation and the distortion is minimized by an optimization process. Later on, other authors formulate the problem using polyphase transfer matrix and are able to obtain PR cosine-modulated filter banks [15, 16, 17, 53].

Soman et al. [18] present the theory and lattice structure for M-channel linear-phase orthogonal filter bank. They show that filter banks with both orthogonality and linear-phase properties can exist when $M \geq 4$. DeQueiroz et al. [19] introduce GenLOT as an alternative factorization where the lattice structure is a generalization of the Discrete Cosine Transform (DCT) and Lapped Orthogonal Transform (LOT) [15].

The wavelet transform is an octave-band representation for signals; the discrete wavelet transform may be obtained by iterating an M-channel filter bank on its lowpass output (see Figure 2 for dyadic wavelet transform) [20]. This multiresolution decomposition of a signal into its coarse and detail components is useful for data compression, feature extraction, and denoising. In the case of images, the wavelet representation is well-matched to psychovisual models, and compression systems based on the wavelet transform yield perceptual quality superior to other methods for a given compression ratio [42, 43, 44]. Furthermore, the multiresolution nature of the wavelet transform enables fast browsing of image databases (the user may reconstruct only the coarsest scale of an image to decide whether he/she wants to examine it at a finer resolution). For audio compression, tree structures similar to the wavelet representation can be used to mimic the critical bands of human audition within the subband decomposition [21, 22].

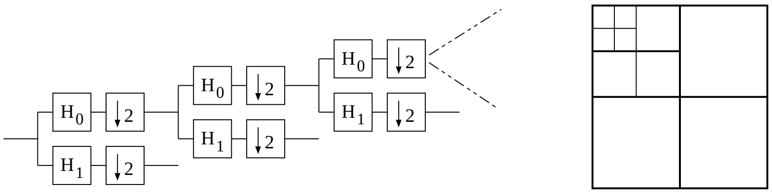

Figure 2: Discrete dyadic wavelet transform (from iteration of a 2-channel filter bank)

II. Theory of Two-channel Perfect-Reconstruction Filter Bank

Consider the two-channel maximally-decimated filter bank where the lengths of $H_0(z)$ and $H_1(z)$ are N_0 and N_1, respectively. The input-output relation is:

$$\widehat{X}(z) = T_0(z)X(z) + T_1(z)X(-z) \tag{1}$$

where $T_0(z) = \frac{1}{2}(F_0(z)H_0(z) + F_1(z)H_1(z))$ and $T_1(z) = \frac{1}{2}(F_0(z)H_0(-z) + F_1(z)H_1(-z))$. The transfer function $T_0(z)$ and $T_1(z)$ are the *distortion* and *aliasing* transfer functions of the system. The objective in designing a perfect reconstruction (PR) filter bank is to find $H_k(z)$ and $F_k(z)$ such that the input is a delayed copy of the output. In other words, the filters have to satisfy the following conditions:

$$F_0(z)H_0(z) + F_1(z)H_1(z) = z^{-n_0} \qquad F_0(z)H_0(-z) + F_1(z)H_1(-z) = 0. \tag{2}$$

The second equation (aliasing-free condition) implies that $F_0(z) = H_1(-z)$, $F_1(z) = -H_0(-z)$. One can verify that n_0 must be an odd integer and the product polynomial $P(z) = F_0(z)H_0(z)$ is a halfband filter of length $N_0 + N_1 - 1$. Assuming that $P(z)$ is a linear-phase halfband filter, then $N_0 + N_1 = 4\ell$, ℓ is a positive integer. The above condition on the filter lengths holds for all two-channel PR FIR filter bank, where $P(z)$ is a linear-phase function.

In addition to the above PR conditions, which are based on the transfer functions $H_0(z)$ and $H_1(z)$, one could also derive the equivalent conditions that are based on the impulse responses $h_k(n)$ and $f_k(n)$ and conditions that are based on the polyphase transfer matrices $\mathbf{E}(z)$ and $\mathbf{R}(z)$. These equivalent conditions are [24, 25]:

$$\sum_n h_k(n)\, f_\ell(2m-n) = \delta(m)\,\delta(k-\ell) \qquad \mathbf{R}(z)\,\mathbf{E}(z) = z^{-n_0}\,\mathbf{I} \quad \text{or} \quad z^{-n_0}\begin{bmatrix} 0 & 1 \\ z^{-1} & 0 \end{bmatrix}.$$

2.1. Paraunitary Filter Bank In the case of paraunitary (orthogonal) filter bank, the filter lengths are equal ($N_0 = N_1 = N =$ even integer) and the synthesis filters are the time-reversed versions of the analysis filters, i.e., $F_k(z) = z^{-(N-1)}H_k(z^{-1})$. The product filter simplifies to $P(z) = z^{-(N-1)}H_0(z^{-1})H_0(z)$. In summary, the two-channel paraunitary filter bank has the following properties:

$$\begin{cases} H_0(z) \text{ is a spectral factor of a halfband filter} \\ H_1(z) = -z^{-(N-1)}H_0(-z^{-1}), \quad F_k(z) = z^{-(N-1)}H_k(z^{-1}). \end{cases} \tag{3}$$

Given a maxflat filter $P(z)$ with length $2N-1$ [24], i.e.,

$$P(z) = z^{-N}\left(\frac{1+z^{-1}}{2}\right)^{2N}\sum_{\ell=0}^{N-1} 2\binom{N+\ell-1}{\ell}(-z)^{\ell}\left(\frac{1-z^{-1}}{2}\right)^{2\ell}, \tag{4}$$

one can find its spectral factor by either finding the zeros of $P(z)$ directly or by the method of [26]. The corresponding wavelets has $N/2$ vanishing moments and the scaling function can be used to approximate any polynomial of degree less than N [20], [23]. Figure 3(a) shows the magnitude responses of an orthogonal filter bank with length 8. It is the minimum-phase spectral factor of a maximally-flat halfband filter of length 15.

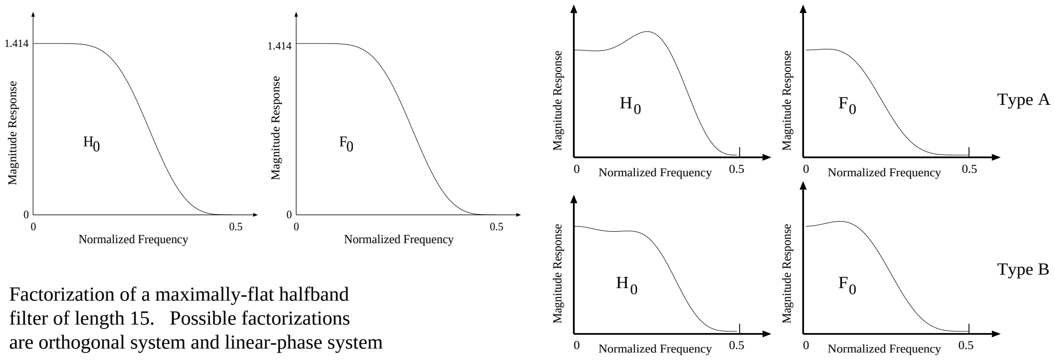

Figure 3: Magnitude responses of (a). maximally-flat orthogonal filter bank with length 8, (b). Type A linear-phase filter bank of length $(8,8)$ and (c). Type B linear-phase filter bank of length $(9,7)$.

The above paraunitary filter bank can also be realized in a lattice structure as shown in Fig. 4(a) where $\mathbf{U}_k = \begin{bmatrix} \cos\theta_k & \sin\theta_k \\ -\sin\theta_k & \cos\theta_k \end{bmatrix}$ and Fig. 4(b) where $\mathbf{V}_k = \begin{bmatrix} 1 & \alpha_k \\ \alpha_k & 1 \end{bmatrix}$, $\beta = 1/\sqrt{\prod 1+\alpha_k^2}$. The lattice structure is complete. For any choices of θ_k (or α_k), the resulting filters are paraunitary, and given any paraunitary filter bank, there exists a unique set θ_k (or α_k) that implement it. For example, the D_6 wavelet has lattice angles $\theta_0 = \frac{\pi}{3}$ and $\theta_1 = -\frac{\pi}{12}$. Given $H_0(z)$, the procedure to synthesize θ_k (or α_k), is derived in [3]. Since the above lattice structure covers all two-channel paraunitary filter bank, one can find the appropriate set of angles θ_k or lattice coefficients α_k that optimizes a certain error measure.

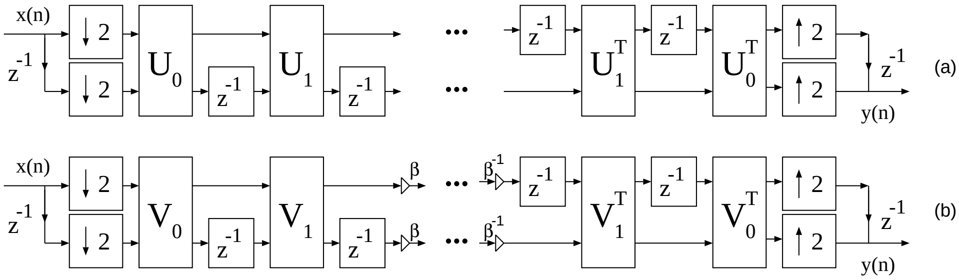

Figure 4: Factorization of two-channel paraunitary filter bank.

2.2 Biorthogonal Linear-Phase Filter Bank: In this section, we discuss the theory and lattice structures of the two-channel biorthogonal linear-phase filter banks. Let $H_k(z)$ and $F_k(z)$ be the linear-phase analysis and synthesis filters of a two-channel system. (Recall that a linear-phase filter $H(z)$ of length N satisfies the self-symmetry property: $H(z) = \pm z^{-(N-1)}H(z^{-1})$; $h(n) = \pm h(N-1-n)$.) Table 1 shows the two possible choices for N_0 and N_1. For Type A, both filter must have even lengths and the length difference is a multiple of 4. For Type B, both filters have odd lengths and the length difference is $4K+2$.

The next point addresses the symmetric polarities of the filters. $P(z)$ is a symmetric lowpass halfband filter and $P(z) = F_0(z)H_0(z)$, therefore both $F_0(z)$ and $H_0(z)$ must also be symmetric lowpass filters, since antisymmetric filters can not be lowpass. Based on the aliasing-cancellation condition, one can deduct the symmetric polarities for $H_1(z)$ and $F_1(z)$. Table 1 summarizes the lengths and symmetry polarities of both types of linear phase filter banks.

	N_0	N_1	$H_0(z)$ & $F_0(z)$	$H_1(z)$ & $F_1(z)$
Type A	$2L$	$2L+4K$	Symmetry	Anti-symmetry
Type B	$2L+1$	$2L+4K+3$	Symmetry	Symmetry

Table 1. Two types of PR linear-phase filter banks.

Given any Type A pair of filters $(H_0(z), H_1(z))$, its polyphase transfer matrix $\mathbf{E}(z)$ can be factorized as

$$\mathbf{E}(z) = (DFT)\,\Gamma_{L-1}\Lambda(z)\Gamma_{L-2}\Lambda(z)\ldots\Lambda(z)\Gamma_0 \qquad \Gamma_k = \begin{pmatrix} 1 & \gamma \\ \gamma & 1 \end{pmatrix}, \quad \Lambda(z) = \begin{pmatrix} 1 & 0 \\ 0 & z^{-1} \end{pmatrix}$$

where DFT is a two-point DFT matrix. Let N ($N = 2J$) be the length of $H_0(z)$, then the number of lattice sections Γ_k in the analysis bank is J. Each lattice section requires 2 multiplications and 2 additions, which implies that the number of multiplications and additions at the analysis bank is $2J$ and $2J$, respectively. The effective computation complexity (at the input rate) is J multiplications and J additions. An alternative implementation uses one multiplication and three additions per lattice section.

Given any Type B pair of filters $(H_0(z), H_1(z))$, its polyphase transfer matrix $\mathbf{E}(z)$ can be factorized as

$$\mathbf{E}(z) = \mathbf{D}_{\alpha_0,\alpha_1}\prod_{k=2}^{L}\mathbf{A}_k(z), \quad \mathbf{A}_k(z) = \begin{bmatrix} 1+z^{-1} & 1 \\ 1+\beta_k z^{-1}+z^{-2} & 1+z^{-1} \end{bmatrix}\begin{bmatrix} \alpha_k & 0 \\ 0 & 1 \end{bmatrix}, \quad \mathbf{D}_{\alpha_0,\alpha_1} = \begin{bmatrix} \alpha_0 & 0 \\ 0 & \alpha_1 \end{bmatrix}.$$

In a practical system, it is sufficient to set all β_k equals to 0, except for β_2. This would help speeding up the implementation of Type B system. Procedure to find α_k and β_2 can be found in [6, 7].

Given a linear-phase halfband maxflat filter $P(z)$, there are many ways of distributing its zeros such that both $F_0(z)$ and $H_0(z)$ are linear-phase filters. Consider the case where $P(z)$ has length 15, it can be factorized into several Type-A systems, when $(N_0, N_1) = \{(8,8),\ (10,6),\ (12,4),\ (14,2),\ \text{etc.}\}$. Similarly for Type B system, $P(z)$ can be factorized such that $(N_0, N_1) = \{(9,7),\ (11,5),\ (13,3),\ \text{etc.}\}$. The main difference between these systems are the number of zeros at $\omega = \pi$ (i.e., vanishing moments). Figure 3(b) shows the frequency responses of $H_0(z)$ and $F_0(z)$ for both types of linear-phase system. The filters in Type A have lengths $(8,8)$ whereas they have lengths $(9,7)$ in Type B system.

2.3. Design Methods: Distributing the zeros of $P_0(z)$: Given a polynomial of the form $P(z) = F_0(z)H_0(z)$, the objective here is to find the two unknown polynomials $F_0(z)$ and $H_0(z)$. We assume that all polynomials have real-coefficients in the discussion below. Note that in a paraunitary filter bank, $F_0(z) = z^{-(N-1)}H_0(z^{-1})$, and the above problem becomes the problem of finding spectral factor $H_0(z)$. For a low-degree polynomial $P(z)$, one can find its zeros and distribute them to $F_0(z)$ and $H_0(z)$. Since all polynomials are real-valued, the zeros have to be grouped in complex-conjugate pairs.

For example, suppose that $P(z)$ has 10 zeros as shown in Fig. 5, then there are many ways of distributing its zeros to $F_0(z)$ and $H_0(z)$. Note that all zeros of $H_0(z)$ in Fig. 5(a) are inside (and on unit circle), therefore this is a minimum-phase factorization. Similarly all zeros of $F_0(z)$ in Fig. 5(b) are outside (and on the unit circle), it is therefore a maximum-phase factorization. In the other hands, both $F_0(z)$ and $H_0(z)$ in Fig. fig:polezero-iscas(b) have zeros inside and outside the unit circle. Moreover, the zeros are chosen such that $F_0(z)$ and $H_0(z)$ are linear-phase filters (symmetric polynomials). The above two factorizations demonstrate the essential ideas in designing two-channel paraunitary filter bank (orthogonal wavelets) and two-channel linear-phase filter bank (symmetric wavelets).

2.4. Other Design Methods: Finding zeros of a high-degree polynomial is difficult. In the case of paraunitary filter bank ($F_0(z) = z^{-(N-1)}H_0(z^{-1})$), the algorithm by Mian and Nainer [26] is widely used. It computes the minimum-phase spectral factor without finding the zeros of $P(z)$. Other design methods includes the lattice-structured approach [3], time-domain approach [29], the quadratic-constrained least-squares approach [27] and the Lagrange-multipler based approach [34, 35].

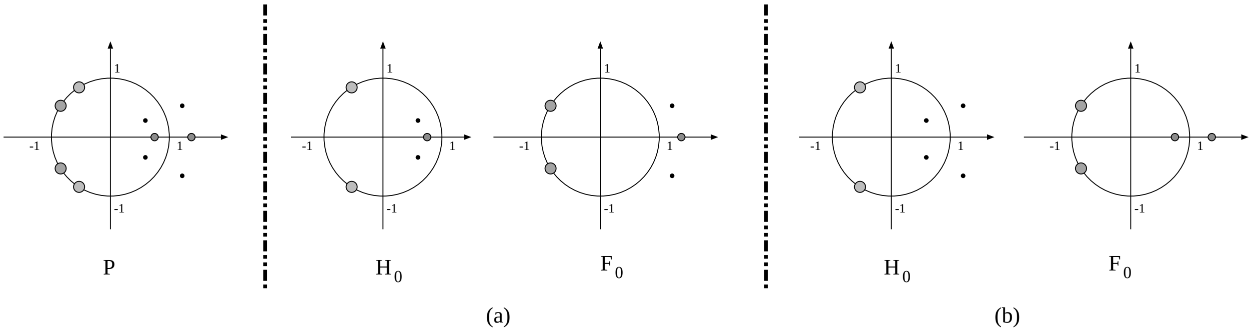

Figure 5: Zero pattern of $P(z)$ and the zero distributions of $F_0(z)$ and $H_0(z)$.

The lattice structure approach is based on the lattice structure implementation of the filter bank where the unknown parameters are the lattice coefficients k_i. Since all PR filter banks are characterized by the appropriate set of lattice coefficients, therefore, the PR conditions are satisfied automatically as long as the search space is constrained only to the lattice coefficient space. The design problem reduces to finding the lattice coefficient such that the objective function is minimized.

For any set of lattice coefficients, the corresponding filters can be computed. The filters are a nonlinear function with respect to the lattice coefficients. Consequently, the objective function (which is normally a function of the filter coefficients) is also a nonlinear function with respect to the lattice coefficients. Thus, designing filter banks with small objective function is a problem because of the nonlinear relation between the lattice coefficients and the objective function.

The time-domain approach formulates the PR conditions in terms of matrices and the filter coefficients [29]. It uses optimization algorithm iteratively to solve (2). The quadratic-constrained approach formulates both the objective function Φ and the PR conditions in the quadratic forms $\mathbf{h}^t\mathbf{P}\mathbf{h}$ and $\mathbf{h}\mathbf{Q}_k\mathbf{h} = c_k$, respectively. The design problem becomes

$$\text{Minimize} \quad \mathbf{h}^t\mathbf{P}\mathbf{h} \quad \text{subject to} \quad \mathbf{h}\mathbf{Q}_k\mathbf{h} = c_k \tag{5}$$

where $\mathbf{h}$ is the coefficients to be found. The advantage of this approach is that the derivatives and the Hessian of both the objective function and the PR conditions can be computed exactly, which helps the minimization algorithm [27].

2.5. Other two-channel PR filter banks: Other two-channel PR filter banks are:

- Biorthogonal filter bank with integer coefficients (sum and difference of 2^{-k}) [30].
- Lagrange-multiplier based approach [34, 35].
- LMS-based algorithm [37].
- Biorthogonal linear-phase filter bank [31, 32].
- Alias-free two-channel allpass-based IIR filter bank [33, 24].
- Alias-free two-channel allpass-based IIR filter bank with linear-phase frequency responses [36].

III. Discrete Dyadic Wavelets

The discrete wavelet transform is obtained by iterating an M-channel multirate filter bank on its lowpass output. The wavelet transform with symmetric basis functions has recently emerged as the next-generation standard for still-image compression. Wavelet methods outperform the current JPEG standard at low bitrates, and degrade gracefully with decreasing bitrate. These advantages are attributed to the underlying multiresolution structure and the smoothness of the basis functions (number of vanishing wavelet moments). Besides its popularity in image compression, wavelets and filter banks are also used in other applications, including high-fidelity audio compression, frequency-domain/time-domain multiplexing, adaptive filtering, transient analysis and detection and denoising.

A *wavelet* decomposition arises from iteration of the lowpass filtering and decimation steps of a multirate filter bank. For a true wavelet, one iterates on the lowpass output only, whereas for a wavelet-packet decomposition, one may iterate on any output. A finite number of iterations will lead to a discrete-time multiresolution analysis with lowpass frequency response $\prod_{k=1}^{n} H_0\left(\frac{\omega}{2^k}\right)$. If the lowpass filter h_0 satisfies the orthonormality constraint and "one vanishing moment" (approximation of order 1): $\sum_k h_0[k] = \frac{1}{\sqrt{2}}$, then the infinite product $\lim_{n\to\infty} \prod_{k=1}^{n} H_0\left(\frac{\omega}{2^k}\right)$

converges to a continuous-time function $\hat{\phi}(\omega)$, whose inverse Fourier transform $\phi(t)$ is called the scaling function. The scaling function $\phi(t)$ and the wavelet $\psi(t)$ are solution of the dilation equations

$$\phi(t) = \sum_k h_0(k)\phi(2t-k)\ , \qquad \psi(t) = \sum_k h_1(k)\phi(2t-k)$$

and it is orthogonal to its integer translates (under mild additional assumptions). If the filter $h_0(n)$ is FIR, then $\phi(t)$ and $\psi(t)$ have compact support. The set of dilates and translates

$$\left\{\psi(2^k t - \ell)\right\}_{k,\ell \in \mathbf{Z}}$$

form a tight frame (and in most cases an orthonormal basis) for $L^2(\mathbf{R})$ [50, 51, 52]. The span of integer translates of the scaling function $\phi(t)$ is the "lowpass" space V_0, the set of *scale-limited signals* [47]. Any continuous-time function $f(t)$ in V_0 can be expanded as a linear combination

$$f(t) = \sum_n v_n^{(0)}\phi(t-n)\ . \qquad (6)$$

The superscript (0) denotes an expansion "at scale level 0." $f(t)$ is completely described by the sequence $\left\{v_n^{(0)}\right\}$. Given such a sequence, its coarse approximation (component in V_1) is computed with the lowpass filter of the wavelet filter bank:

$$v_n^{(1)} = \left(\left(v^{(0)} * h_0\right) \downarrow 2\right)[n]\ .$$

Analogously, the details $w_n^{(1)}$ in $V_0 \ominus V_1$ are computed with the highpass filter $h_1(n)$. Hence, if we take a discrete sequence v_n to be the coefficients of a signal $f(t)$ at some fixed scale, the discrete wavelet transform of v_n will decompose the underlying signal f into a coarse-scale component and detail at several intermediate scales. This decomposition matches multiresolution models of human and computer vision [48], and proves to be an effective transform for high-quality image compression.

Figure 6 shows the orignal image "Lenna" and the its decomposition (three levels decomposition) using the two-channel biorthogonal filter banks with $(9,7)$ coefficients. The block at the upper left corner is a coarse approximation of the original image and the other subbands are details at various scales. Since the filters have several vanishing moments, the signal energy at the subbands are small. Consequently, they have to be amplified in order to see the details.

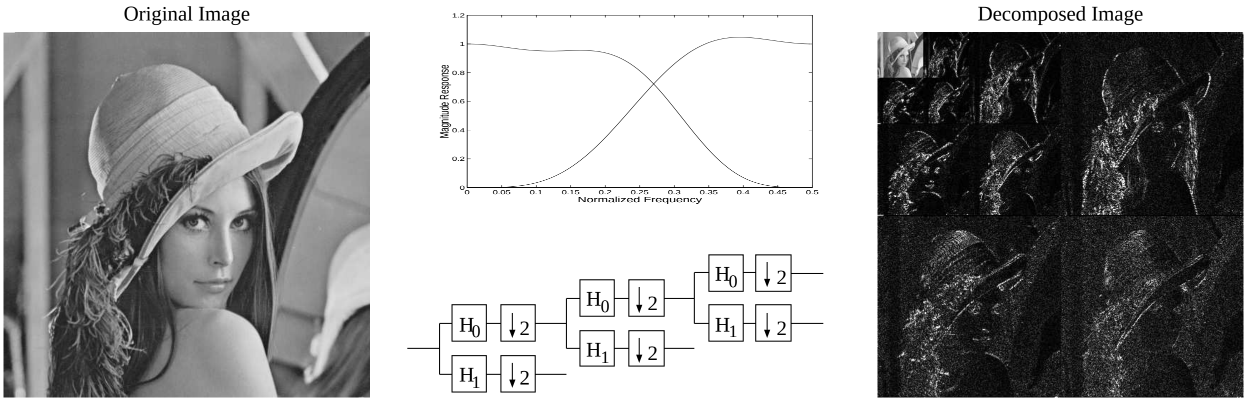

Figure 6: Original image "Lenna" and its multiresolution decomposition. The filter bank used is the $(9,7)$-tap linear-phase filter bank.

Figure 7 shows the frequency responses of the lowpass filters $H_0(z)$, $F_0(z)$ and their corresponding scaling functions for both Type A and Type B linear-phase filter banks. As with any signal processing structure, one must consider the performance of the filters involved. In the case of the wavelet transform, one is concerned with the smoothness of the iterated lowpass filter. Indeed, should one use a wavelet for lossy transform-based image coding, then any quantization noise will appear in the decompressed image as linear combinations of the wavelet transform basis functions. If these basis functions (which are derived from the iterated discrete filter) are not smooth, then perceptually unacceptable artifacts will result.

Strang [23] observed that the N-th order vanishing of wavelet moments is equivalent to polynomial approximation properties of the associated scaling function – if a wavelet system has N vanishing moments, then polynomials of degree less than N lie in the scale-limited space V_0; in other words, they may be represented as a linear combination of translates of the scaling function. In the setting of digital filter banks, this means that any polynomial component of a signal (of degree less than N) is preserved by the lowpass filter and zeroed out by the highpass filter – so long as the wavelet system has N vanishing moments. These smoothness-under-iteration and polynomial approximation properties help explain why wavelet filters with vanishing moments perform so well in image compression. After quantization (which usually gives many bits to the lowpass component), reconstruction artifacts are smooth while locally linear and quadratic information is preserved. Section V presents ECG and image compression examples.

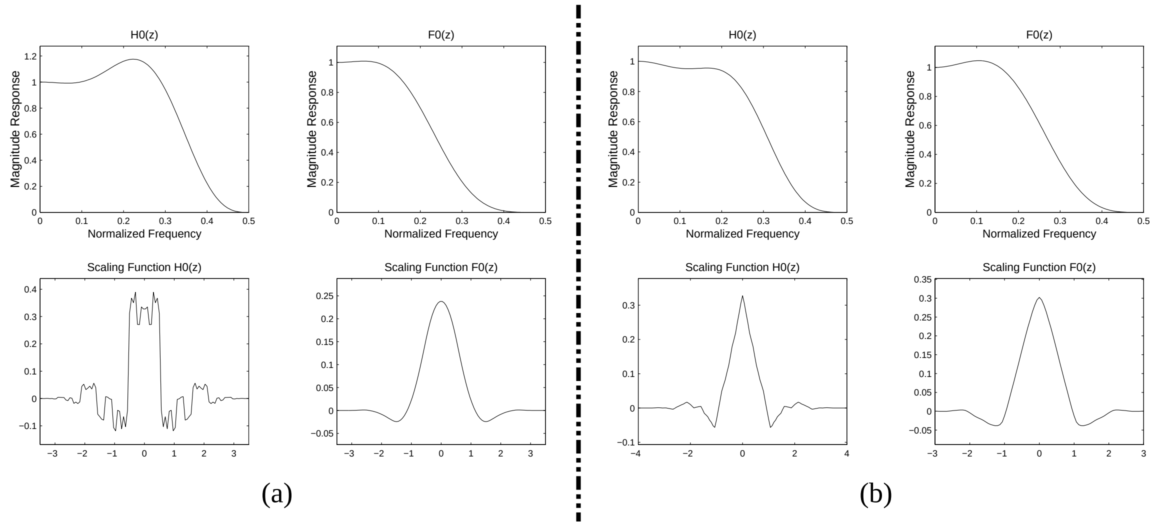

Figure 7: Symmetric wavelets. Magnitude response plots of $H_0(z)$ and $F_0(z)$ amd their corresponding scaling functions. (a). Symmetric dyadic wavelets with $(8,8)$ taps with 3 and 5 vanishing moments, respectively and (b). Symmetric dyadic wavelets with $(9,7)$ taps with 4 vanishing moments each.

IV. M-channel Filter Banks and Wavelets

The corresponding PR conditions for M-channel filter bank are:

$$\begin{cases} T_0(z) = z^{-m_0}, \ T_k(z) = 0, \ k \neq 0; & \text{Based on transfer functions} \\ \mathbf{R}(z)\,\mathbf{E}(z) = z^{-n_0} \begin{bmatrix} \mathbf{0} & \mathbf{I}_{M-r} \\ z^{-1}\mathbf{I}_r & \mathbf{0} \end{bmatrix} & \text{Based on polyphase transfer matrices} \\ \displaystyle\sum_n h_k(n)\, f_\ell(Mm-n) = \delta(m)\,\delta(k-\ell) & \text{Based on impulse responses.} \end{cases}$$

where $T_k(z) = \frac{1}{M}\sum_{\ell=0}^{M-1} F_\ell(z)\,H_\ell(zW^k)$ where $W = e^{-j2\pi/M}$. $T_0(z)$ is the (amplitude and phase) distortion transfer function whereas the remaining transfer functions $T_1(z), \ldots, T_{M-1}$ are aliasing transfer functions. The above three PR conditions are equivalent.

For a given filter length, the number of filter coefficients to be found is directly proportional to the number of channels (M). The design process to find the filters that satisfy the PR conditions is a nonlinear optimization problem. Good solution for filter banks with a large number of parameters is very difficult to find. One needs to impose explicit relation among the filters in order to reduce the number of parameters. Besides the paraunitary properties, other properties include cosine-modulation [15, 16, 17], linear-phase [18, 19, 38, 39] and pairwise-mirror-image [18, 40, 41].

One has to be careful when imposing explicit relations on a filter bank since the chosen relations might prevent the design methods from finding a good solution. For example, we know that the only two-channel linear-phase paraunitary filter bank is the Haar wavelet ($H_0(z) = 1+z^{-1}, \ H_1(z) = 1-z^{-1}$). By imposing both the paraunitary and linear-phase properties, we have limited our solution to a very simple one. The choices of filter banks depend on the applications. For example, cosine-modulated filter bank is used frequently in audio compression and telecommunications because of its efficient implementation and high stopband attenuation. In the other hand, linear-phase filter bank is used in applications where phase informations are important such as in image compression and signal detection.

4.1. Paraunitary filter bank

Paraunitary filter bank is a special case of biorthogonal filter bank where the polyphase transfer matrices $\mathbf{H}(z)$ and $\mathbf{R}(z)$ are related as:

$$\mathbf{R}(z) = \mathbf{E}^{-1}(z) = \widetilde{\mathbf{E}}(z) = z^{-K}\mathbf{E}^{\dagger}(z^{-1}). \tag{7}$$

Consequently, the synthesis filters $F_k(z)$ are related to analysis filters $H_k(z)$ (of length N) as:

$$F_k(z) = z^{-N} H_k(z^{-1}), \qquad f_k(n) = h_k(N-n). \tag{8}$$

When $\mathbf{E}(z)$ are constant matrices, then both $\mathbf{E}(z)$ and $\mathbf{R}(z)$ are unitary matrices. Examples are the DFT, DCT and orthogonal matrices. The two-channel orthogonal filter bank in section 2.1 is a paraunitary filter bank. The corresponding PR condition on the impulse responses is:

$$\sum_n h_k(n)\, h_\ell(Mm+n) = \delta(m)\,\delta(k-\ell).$$

• *Lattice structure*: Let L be the McMillan degree of a causal FIR paraunitary matrix $\mathbf{E}(z)$. $\mathbf{E}(z)$ can be factorized using either Givens rotations [45] or Householder matrices [24, 46]. These lattice structures are complete in the sense that they cover all paraunitary filter bank. Given any paraunitary matrix $\mathbf{E}(z)$, there exists a set of Givens rotation angles or Householder matrices that realizes it.

4.2. Cosine-modulated filter bank

Let $H(z)$ and $F(z)$ be the prototype filters of the analysis and synthesis banks, respectively (as shown in Fig. 8(a)). The cosine-modulated analysis and synthesis filters $H_k(z)$ and $F_k(z)$ are defined as:

$$\begin{cases} H_k(z) = & a_k b_k U_k(z) + a_k^* b_k^* U_k^*(z), \\ F_k(z) = & a_k^* b_k V_k(z) + a_k b_k^* V_k^*(z) \end{cases} \quad \begin{cases} U_k(z) = & H(zW^{k+\frac{1}{2}}), \\ V_k(z) = & F(zW^{k+\frac{1}{2}}), \end{cases} \quad \begin{cases} a_k = & e^{j(-1)^k \frac{\pi}{4}}, \\ b_k = & W^{-\frac{1}{2}(k+\frac{1}{2})}. \end{cases} \tag{9}$$

where $W = e^{-j\frac{k\pi}{M}}$. The analysis and synthesis filters are cosine-modulated versions of the prototype filters, i.e.,

$$\begin{cases} h_k(n) = & 2h(n)\cos(\frac{\pi}{M}(k+\frac{1}{2})(n+\frac{1}{2}-\frac{N}{2}) + (-1)^k\frac{\pi}{4}), \\ f_k(n) = & 2f(n)\cos(\frac{\pi}{M}(k+\frac{1}{2})(n+\frac{1}{2}-\frac{N}{2}) - (-1)^k\frac{\pi}{4}). \end{cases} \tag{10}$$

Clearly from the above equations, the only parameters to be found are $h(n)$ and $f(n)$, $0 \le n \le N-1$. In the subsections below, we will elaborate on the Pseudo-QMF bank and the paraunitary cosine-modulated filter bank.

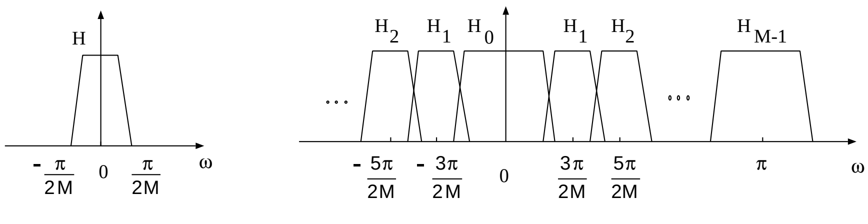

Figure 8: Ideal frequency response of the (a). prototype filter and (b). the analysis filters.

Pseudo-QMF Bank: The above form of $\theta_k = (-1)^k\frac{\pi}{4}$ is suggested by Rothweiler [14] to cancel aliasing error from the adjacent subbands ($T_1(z) \approx 0$). The other aliasing errors in $T_2(z), T_3(z)$, etc. are minimized by constraining the stopband cutoff frequency ω_c of $H(z)$ such that there is no overlap between $H_k(z)$ and $H_{k\pm 2}(z)$. The corresponding condition on ω_c is $\omega_c \le \frac{\pi}{M}$. Consequently, the aliasing error is comparable to the stopband attenuation of the prototype filter $H(z)$. Thus, one could minimize the aliasing error by designing $H(z)$ with high stopband attenuation. The distortion function $T_0(z)$ is not a delay. The design procedure is to find a prototype filter that minimizes the following weighted objective function:

$$\alpha \int_{\omega_s}^{\pi} \left| H(e^{j\omega}) \right|^2 d\omega + (1-\alpha) \int_{0}^{\pi} \left| T_0(e^{j\omega}) - e^{-jn_0\omega} \right|^2 d\omega$$

where $0 \leq \alpha \leq 1$. One often has to trade off aliasing with distortion in the Pseudo-QMF banks.

Near-Perfect-Reconstruction (NPR) Pseudo-QMF Bank: The main different between the NPR Pseudo QMF bank and the Pseudo QMF bank is that the prototype filter $H(z)$ in the NPR Pseudo QMF bank is a *linear-phase spectral factor of a $2M$th band filter*. A consequent of this is $T_0(z) = z^{-n_0}$, i.e., there is no distortion. The only error are the aliasing errors from $T_2(z), \ldots, T_{M-2}(z)$ which can be minimized by designing a filter $H(z)$ with high attenuation. In summary, if we know how to a find a linear-phase spectral factor of an $2M$th band filter with high attenuation, then there is no distortion at the output. The only error is aliasing. They are comparable to the stopband attenuation of $H(z)$.

Figure 9 shows the frequency responses of a 16-channel NPR cosine-modulated filter bank. The filter length is 256. By constraining $H(z)$ to be the spectral factor of a 32-band filter, the resulting filter bank has no magnitude nor phase distortion. The only distortion here is the aliasing, which is less than or equal to -72 dB.

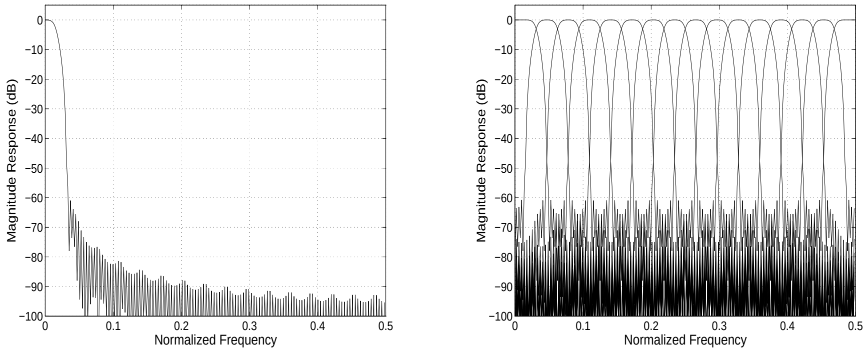

Figure 9: Frequency response plots for the 16-channel NPR cosine-modulated filter bank (a). Prototype filter $H(z)$. (b). Analysis filters $H_k(z)$.

Paraunitary Cosine-Modulated Filter Bank: Let $H(z) = \sum_{\ell=0}^{2M-1} z^{-\ell} G_\ell(z^{2M})$ be the linear-phase prototype filters where $G_\ell(z)$ is the Type-I polyphase components of $H(z)$. $\mathbf{E}(z)$ can be expressed in terms of $G_\ell(z)$ and $\widehat{\mathbf{C}}$ as [17]

$$\mathbf{E}(z) = \widehat{\mathbf{C}} \begin{bmatrix} \mathbf{g}_0(-z^2) \\ z^{-1}\mathbf{g}_1(-z^2) \end{bmatrix}, \quad \begin{cases} \mathbf{g}_0(z) = \text{diag} \begin{bmatrix} G_0(z) & G_1(z) & \ldots & G_{M-1}(z) \end{bmatrix} \\ \mathbf{g}_1(z) = \text{diag} \begin{bmatrix} G_M(z) & G_{M+1}(z) & \ldots & G_{2M-1}(z) \end{bmatrix} \\ \left[\widehat{\mathbf{C}}\right]_{k,\ell} = 2\cos\left(\frac{\pi}{M}(k+\frac{1}{2})(n+\frac{1}{2}-\frac{N}{2}) + (-1)^k \frac{\pi}{4} \right). \end{cases}$$

Using the above $\mathbf{E}(z)$, one obtains the expression for $\mathbf{P}(z) \triangleq \widetilde{\mathbf{E}}(z)\mathbf{E}(z)$ as follows

$$\mathbf{P}(z) = \begin{bmatrix} \widetilde{\mathbf{g}_0}(-z^2) & z\widetilde{\mathbf{g}_1}(-z^2) \end{bmatrix} \widehat{\mathbf{C}}^t \widehat{\mathbf{C}} \begin{bmatrix} \mathbf{g}_0(-z^2) \\ z^{-1}\mathbf{g}_1(-z^2) \end{bmatrix} \tag{11}$$

Substitute the appropriate expression for $\widehat{\mathbf{C}}^t\widehat{\mathbf{C}}$ and simplifying, equation (11) becomes (for length $= 2mM$)

$$\widetilde{G}_\ell(z)G_\ell(z) + \widetilde{G}_{M+\ell}(z)G_{M+\ell}(z) = \frac{1}{2M}(-z)^{-s}. \tag{12}$$

In summary, as long as the polyphase components $G_\ell(z)$ of the linear-phase prototype filter $H(z)$ satisfy the conditions in (12), then the cosine-modulated filter bank is paraunitary.

- *Lattice Structure* : The above condition (12) is the same as the condition in the paraunitary two-channel filter bank. Thus, the cosine-modulated filter bank can be implemented as a parallel bank of two-channel paraunitary filter bank [24, 17]. The implementation is efficient because of the lattice structures associated with the pair $[G_k(z), G_{k+M}(z)]$ and the matrix $\widehat{\mathbf{C}}$. Figure 10 shows the frequency responses of an 8-channel PR cosine-modulated filter bank. The filter length is 128. The resulting filters have stopband attenuation about 80 dB. The design procedure is based on the quadratic-constrained formulation [27].

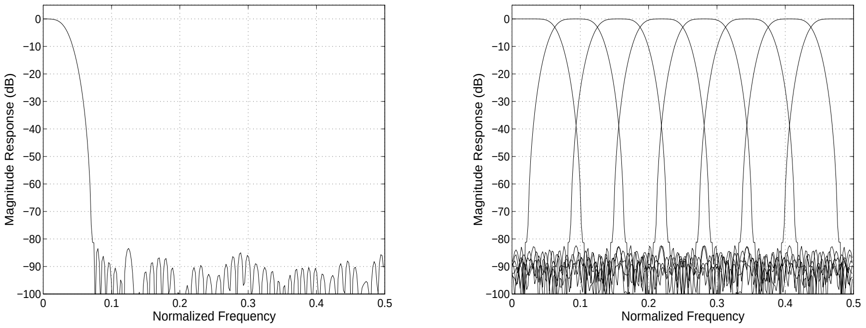

Figure 10: Frequency response plots for an 8-channel PR cosine-modulated filter bank (a). Prototype filter $H(z)$. (b). Analysis filters $H_k(z)$.

Other cosine-modulated filter banks:

- Paraunitary cosine-modulated linear-phase filter bank [54, 55].
- Arbitrary-length paraunitary cosine-modulated filter bank [56, 57, 58].
- Biorthogonal FIR cosine-modulated filter bank [59, 58].
- Biorthogonal IIR cosine-modulated filter bank [60].
- Variable-delay cosine-modulated filter bank [60, 61].

4.3. Linear-phase filter bank

Although linear-phase and paraunitary properties can not be simultaneously imposed in the case of two-channel (except for the case of Haar wavelets), they can coexist for filter banks with more channels. For instance, DCT (Discrete-Cosine-Transform) and LOT (Lapped Orthogonal Transform) are two examples where both the analysis and synthesis filters $H_k(z)$ and $F_k(z)$ are linear-phase FIR filters and the corresponding filter banks are paraunitary. Assuming that M is even, N is a multiple of M ($N = LM$) and $f_k(n) = h_k(N-1-n)$. The number of symmetric and antisymmetric filters is as follows [18]:

$$\begin{cases} \frac{M}{2} \text{ symmetric } \& \ \frac{M}{2} \text{ antisymmetric filters;} & \text{even} M \\ \frac{M+1}{2} \text{ symmetric } \& \ \frac{M-1}{2} \text{ antisymmetric filters;} & \text{odd} M. \end{cases}$$

The polyphase transfer matrix $\mathbf{E}(z)$ of degree $L-1$ can be decomposed as a product of orthogonal matrices and delays,

$$\mathbf{E}(z) = \mathbf{SQT}_{L-1}\Lambda(z)\mathbf{T}_{L-2}\Lambda(z)\cdots\Lambda(z)\mathbf{T}_0\mathbf{Q} \tag{13}$$

where

$$\mathbf{Q} = \begin{bmatrix} \mathbf{I} & \mathbf{0} \\ \mathbf{0} & \mathbf{J} \end{bmatrix}, \qquad \Lambda(z) = \begin{bmatrix} \mathbf{I} & \mathbf{0} \\ \mathbf{0} & z^{-1}\mathbf{I} \end{bmatrix}, \qquad \mathbf{S} = \frac{1}{\sqrt{2}} \begin{bmatrix} \mathbf{S}_0 & \mathbf{0} \\ \mathbf{0} & \mathbf{S}_1 \end{bmatrix} \begin{bmatrix} \mathbf{I} & \mathbf{J} \\ \mathbf{I} & -\mathbf{J} \end{bmatrix}. \tag{14}$$

$\mathbf{S}_0$ and $\mathbf{S}_1$ can be any $M/2 \times M/2$ orthogonal matrices. $\mathbf{T}_i$ are $M \times M$ orthogonal matrices

$$\mathbf{T}_i = \begin{bmatrix} \mathbf{I} & \mathbf{I} \\ \mathbf{I} & -\mathbf{I} \end{bmatrix} \begin{bmatrix} \mathbf{U}_i & \mathbf{0} \\ \mathbf{0} & \mathbf{V}_i \end{bmatrix} \begin{bmatrix} \mathbf{I} & \mathbf{I} \\ \mathbf{I} & -\mathbf{I} \end{bmatrix} \tag{15}$$

where $\mathbf{U}_i$ and $\mathbf{V}_i$ are arbitrary orthogonal matrices. The above factorization in (13) covers all linear-phase paraunitary filter bank for even number of channels. In other words, given any sets of filters $H_k(z)$ that belongs to a linear-phase paraunitary filter bank, one can obtain the corresponding matrices $\mathbf{S}, \mathbf{Q}$ and $\mathbf{T}_k$.

GenLOT: Another factorization for linear-phase paraunitary filter bank is as follows:

$$\mathbf{E}(z) = \mathbf{K}_{L-1}(z)\mathbf{K}_{L-2}(z)\cdots\mathbf{K}_1(z)\mathbf{E}_0 \quad \text{where} \quad \mathbf{K}_i(z) = \Phi_i\mathbf{W}\Lambda(z)\mathbf{W}. \tag{16}$$

where

$$\mathbf{W} = \begin{bmatrix} \mathbf{I} & \mathbf{I} \\ \mathbf{I} & -\mathbf{I} \end{bmatrix}, \quad \Phi_i = \begin{bmatrix} \mathbf{U}_i & \mathbf{0} \\ \mathbf{0} & \mathbf{V}_i \end{bmatrix}, \quad \Lambda(z) = \begin{bmatrix} \mathbf{I} & \mathbf{0} \\ \mathbf{0} & z^{-1}\mathbf{I} \end{bmatrix}, \quad \mathbf{E}_0 = \frac{1}{\sqrt{2}} \begin{bmatrix} \mathbf{S}_0 & \mathbf{0} \\ \mathbf{0} & \mathbf{S}_1 \end{bmatrix} \begin{bmatrix} \mathbf{I} & \mathbf{J} \\ \mathbf{I} & -\mathbf{J} \end{bmatrix}.$$

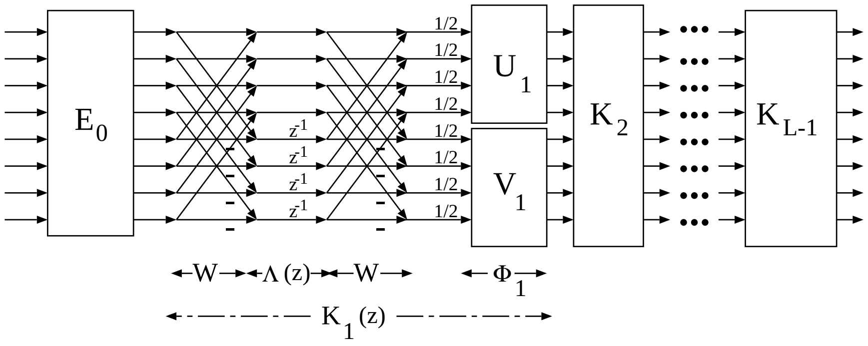

Figure 11: GenLOT - Generalized Lapped Orthogonal Transform.

Figure 11 shows the corresponding lattice structure for GenLOT. Note that the DCT and the LOT are special cases of GenLOT where the length is M and $2M$, respectively. Figure 12(a) and (b) shows the frequency responses of the analysis filters for GenLOT (length 48) and LOT (length 16), respectively. They will be used in the image compression example in section V.

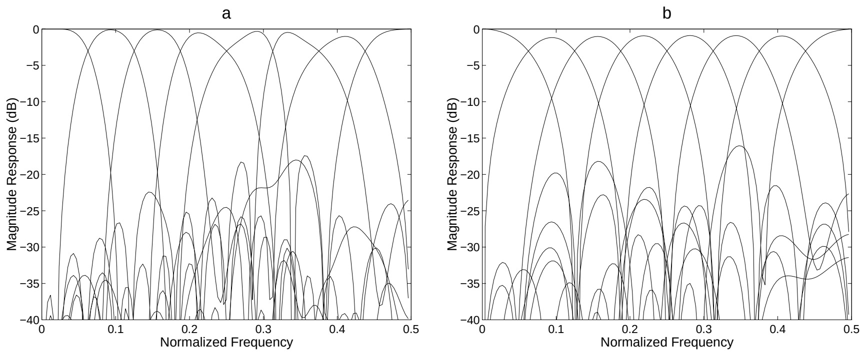

Figure 12: Frequency response plots for the 8-channel (a). GenlOT with length 48 and (b). LOT with length 16.

V. Applications in image and ECG compressions

5.1. Image compression

One of the most successful applications of the wavelet transform is transform-based image compression (also called coding). A transform-based coder (depicted in Figure 13) operates by transforming the data to remove redundancy, then quantizing the transform coefficients (a lossy step), and finally entropy coding the quantizer output. Because of their superior energy compaction properties and correspondence with the human visual system, wavelet compression methods have produced superior objective and subjective results [42, 43, 44]. Because a wavelet basis consists of functions with both short support (for high frequencies) and long support (for low frequencies), large smooth areas of an image may be represented with very few bits, and detail added where it is needed.

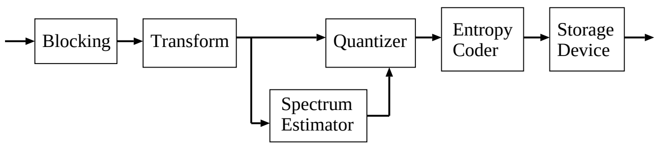

Figure 13: Transform-based coder.

As an example, Figure 14 shows the original image and four reconstructed images, compressed at 64 : 1 compression ration. The bitrate is 0.125 bpp. The texture in this image has a lof of directional information, which is very difficult to compress. At this compression level, many texture details are lost or distorted, as evidenced from the areas in the pant and scarf. For the wavelet-based transform, we use Type A system with $(6, 10)$ taps and Type B system with $(9, 7)$ taps. For the block transform, we use the LOT (8 channel with length 16) and the GenLOT (8 channel with length 48). The accompanied table shows the mean-squared error (MSE), the peak signal-to-noise ratio (PSNR) and the maximum error of the above four transforms.

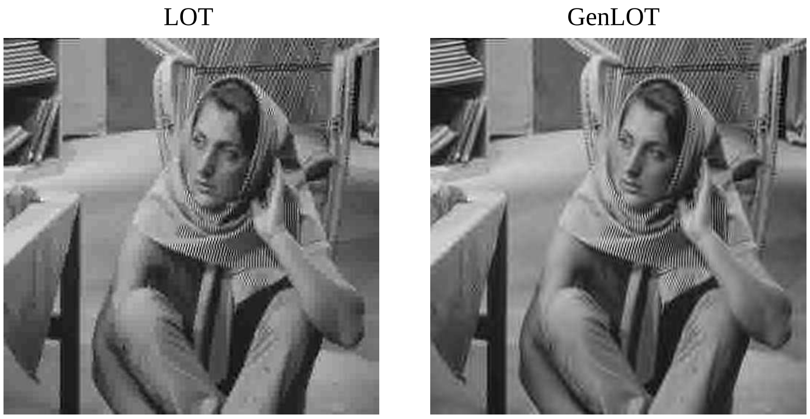

64 : 1 Compression (0.125 bpp)	MSE	PSNR (dB)	Max. Error
Wavelet (6,10)	434.4	21.75	128.5
Wavelet (9,7)	431.1	21.78	155.1
LOT	417.2	21.93	130.3
GenLOT	399.6	22.11	128.6

Figure 14: Image compression example for 0.125 bpp (64 to 1 compression). Original image and four reconstructed images from the wavelet transforms, the Lapped Orthogonal transform (LOT) and the Generalized Lapped Orthogonal transform (GenLOT).

5.2. ECG compression

Electrocardiogram (ECG) waveforms are signals measured from the heart. They provide the cardiologists essential informations about the heart conditions. Normally, the cardiologists needs a 24-hour recording of a patient's ECG in order to detect heart abnormalities or disorders. Storage requirements can range from 26 Mbytes for a system with 1 lead, 12 bit resolution sampled at 200 Hz to 138 Mbytes for a system with 2 leads, 16 bit resolution sampled at 400 Hz. Consequently, there is a need for a low bit rate compression algorithm.

The formance of an ECG compression algorithm is measured by its ability to minimize the distortion while retaining all significant features of the signal. Figure 15 shows the original ECG waveform (dashed line) and the reconstructed waveform (solid line), using wavelet-based compression algorithm. The filter pair used in the compression is the (9,7) taps and the number of levels is 4. The compression ratio is 8 to 1 and the resulting PRD (percentage root-mean-square difference) is 3%. One also notice that the reconstructed signal preserves all of the clinical significant.

Acknowledgements: The author would like to thank Steffen Trautmann and Adriannus Djohan for generating the design examples.

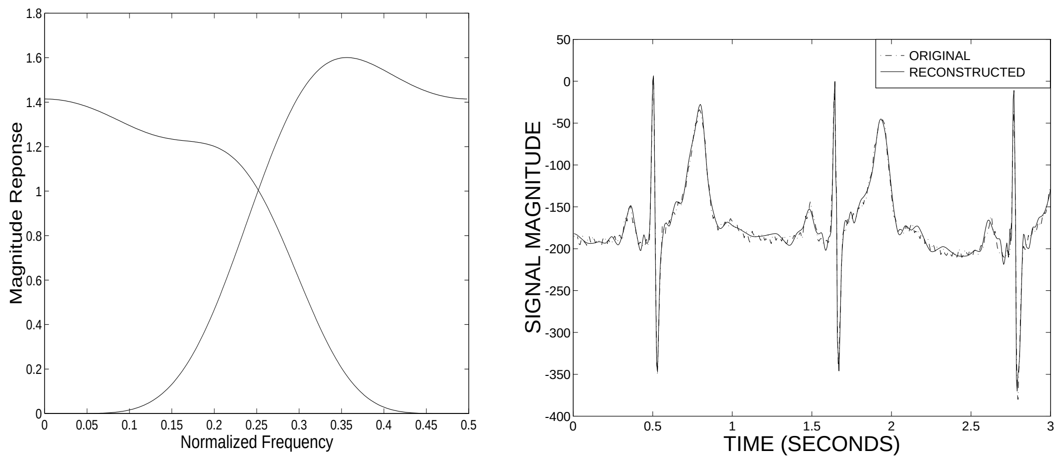

Figure 15: ECG Compression. 8 : 1 compression with $PRD = 3\%$ (a). Magnitude response of the $(13, 11)$-taps linear-phase filter pair. (b). Original and reconstructed signals.

References

[1] M. J. Smith and T. P. Barnwell, III, "A procedure for designing exact reconstruction filter banks for tree structured subband coders," *Proc. IEEE ICASSP*, pp. 27.1.1-27.1.4, March 1984.

[2] Ramstad, T. A., "Analysis/synthesis filter banks with critical sampling," *Int. Conf. on Digital Signal Processing*, Florence, Sept. 1984.

[3] Vaidyanathan, P. P. and Hoang, P. Q., "Lattice structures for optimal design and robust implementation of two-channel perfect-reconstruction QMF banks," *IEEE Trans. on ASSP*, pp. 81-94, Jan. 88.

[4] Vetterli, M., "Filter banks allowing for perfect reconstruction," *Signal Processing*, pp. 219-244, April 86.

[5] Vaidyanathan, P. P., "Theory and design of M-channel maximally decimated quadrature mirror filter wth arbitrary M, having perfect reconstruction property," *IEEE Trans. on ASSP*, pp. 476-492, April 87.

[6] Nguyen, T. Q. and Vaidyanathan, P. P., "Two Channel Perfect Reconstruction FIR QMF Structures which Yield Linear Phase Analysis and Synthesis Filters", *IEEE Trans. on ASSP*, pp. 676-690, May 1989.

[7] Brislawn, C., "A simple lattice architecture for even-order linear-phase perfect reconstruction filter banks," *Proc. IEEE-SP Intl. Symp. Time-Frequency and Time-Scale Analysis,* Philadelphia, PA, 1994, pp. 124-127.

[8] Vetterli, M. and Le Gall, D., "Perfect reconstruction filter banks : some properties and factorizations", *IEEE Trans. ASSP*, pp. 1057–1071, July 1989.

[9] Cohen, A., Daubechies, I. and Feauveau, J.-C., "Biorthogonal Bases of Compactly Supported Wavelets," *Comm. Pure Appl. Math.*, 45 (1992).

[10] Vetterli, M. and Herley, C., "Wavelets and filter banks," *IEEE Trans. on SP*, vol SP-40, 1992.

[11] "Wavelet Scalar Quantization Gray Scale Fingerprint Image Compression Specification," Criminal Justice Information Services, FBI, Washington, DC, 1993.

[12] Dehery, Y. F., Lever, M. and Urcun, P., "A MUSICAM source codec for digital audio broadcasting and storage," *Proc. IEEE ICASSP*, Toronto, Canada, 1991.

[13] Nussbaumer, H. J., "Pseudo QMF filter bank," *IBM Tech. disclosure bulletin*, vol 24, pp. 3081-3087, Nov. 1981.

[14] Rothweiler, J. H., "Polyphase quadrature filters, a new subband coding technique," *Proc. of IEEE ICASSP*, vol 24, pp. 1980-1983, April 1983.

[15] Malvar, H. S. and Staelin, D. H., "Lapped transforms for efficient transform/subband coding," *IEEE Trans. on ASSP*, pp 969-978, June 1990.

[16] Ramstad, T. A., "Cosine-modulated analysis-synthesis filter bank with critical sampling and perfect reconstruction," *Proc. IEEE ICASSP*, pp. 1789-1792, May 1991.

[17] Koilpillai, R. D. and Vaidyanathan, P. P., "Cosine-modulated FIR filter banks satisfying perfect reconstruction," *IEEE Trans. on SP*, pp 770-783, April 1992.

[18] Soman, A. K., Vaidyanathan, P. P. and Nguyen, T. Q., "Linear-phase paraunitary filter banks: theory, factorizations and applications," *IEEE Trans. on SP*, vol. 41, Dec. 1993.

[19] R. de Queiroz, T. Nguyen, and K. Rao, "Generalized Linear-Phase Lapped Orthogonal Transforms," *Proc. IEEE ISCAS*, London, 1994.

[20] Daubechies, I., *Ten Lectures on Wavelets*, CBMS-NSF Series on Applied Mathematics, SIAM, 1992.

[21] Stautner, J., "High Quality Audio Compression for Broadcast and Computer Applications," presented at SMPTE Advanced Television and Electronic Imaging Conference, San Francisco, Feb. 1992 (also Aware Technical Report AD920207).

[22] Brandenburg, K. and Johnston, J., "Second generation perceptual audio coding: the hybrid coder," 88th Audio Engineering Society convention, 1990.

[23] Strang, G., "Wavelets and dilation equations", *SIAM Review,* 31 (1989), pp. 614-627.

[24] Vaidyanathan, P. P., *Multirate Systems and Filter Banks*, Prentice Hall, 1993.

[25] Gopinath R. and Burrus, C. S., "Wavelet transforms and filter banks," *Wavelets and applications*, edited by C. H. Chui, Academic Press, 1991.

[26] Mian, G. A. and Nainer, A. P., "A fast procedure to design equiripple minimum-phase FIR filters," *IEEE Trans. on Circuits and Systems*, May 82.

[27] Nguyen, T. Q., "A quadratic constrained least-squares approach to the design of digital filter banks," *Proc. of ISCAS 92*, San Diego, pp.1344-1347, May 1992.

[28] T. E. Tuncer and T. Q. Nguyen, "General Analysis of Two-Band QMF Banks," *IEEE Trans. on Signal Processing*, Feb. 1995.

[29] Nayebi, K., Barnwell, T. P. III and Smith, M. J. T., "Time-domain filter bank analysis: A new design theory", *IEEE Trans. on SP*, vol. 40, June 92.

[30] Akansu, A. N. and Haddad, R. A., *Multiresolution Signal Decomposition: Transforms, Subbands and Wavelets*, Academic Press, Inc., 1992.

[31] Phoong, S.-M., Kim, C. W., Vaidyanathan, P. P. and Ansari, R., "A new class of two-channel biorthogonal filter banks and wavelet bases" *IEEE Trans. on Signal Processing*, pp. 649-665, March 95.

[32] Kiya H., Yae M. and Iwahashi, M., "A Linear-phase two-channel filter bank allowing perfect-reconstruction" *Proc. IEEE ISCAS*, pp. 951-954, 1992.

[33] Vaidyanathan, P. P. Regalia, P. and Mitra, S. K., "Design of doubly complementary IIR digital filters using a single complex allpass filter, with multirate applications," *IEEE Trans. on Circuits and Systems*, pp. 378-389, April 87.

[34] Abdel-Raheem, R., El-Guibaly and Antoniou, A., "Design of low-delay FIR QMF banks using the Lagrange-multiplier approach," *Electronics Letters*, pp. 924-926, June 94.

[35] Horng, B. R. and Willson, A. N., "Lagrange multiplier approaches to the design of two-channel perfect-reconstruction linear phase FIR filter bank," *IEEE Trans. on Signal Processing*, pp. 364-373, Feb. 92.

[36] Ekanayake, M. M. and Premaratne, K., "Two-channel IIR QMF banks with approximately linear-phase analysis and synthesis filters," *Proc. 28th annual asilomar conference*, Nov. 94.

[37] S. Roy, "Design of linear phase FIR filters using the LMS algorithm", *IEEE Trans. on Signal Processing*, April 1993, pp. 1685-1689.

[38] Saghizadeh P. and Willson, A. N., "A new approaches to the design of three-channel perfect-reconstruction linear phase FIR filter banks," *Proc. ICASSP*, pp. 157-160, April 94.

[39] Nguyen, T. Q., Soman A. K. and Vaidyanthan, P. P., "A Quadratic-Constrained Least-Squares Approach to Linear-Phase Orthonormal Filter Bank Design," *Proc. ISCAS*, pp. 383-386, May 93.

[40] Nguyen, T. Q. and Vaidyanthan, P. P., "Maximally Decimated Perfect Reconstruction FIR Filter Banks with Pairwise Mirror-Image Analysis (and Synthesis) Frequency Responses," *IEEE Trans. on ASSP*, pp. 693-706, May 88.

[41] Gopinath, R. A. and Burrus, C. S., "Unitary FIR filter banks and symmetry," *Technical report CML TR92-17*, August 92.

[42] Brower, B. V. "Low-bit-rate image compression evaluations," *Proc. SPIE*, Orlando, FL, April 4-9 1994.

[43] Majani, E. "Biorthogonal wavelets for image compression", *Proc. of the SPIE, VCIP'94*, Sep. 94.

[44] Trautmann, S. and Nguyen, T., "Comparison of linear-phase perfect-reconstruction filter banks in wavelet-transform-based image compression," *Proc. of Conf. on Information Sciences and Systems*, Feb. 95.

[45] Doganata, Z., Vaidyanathan, P. P. and Nguyen, T. Q., "General Synthesis Procedures for FIR Lossless Transfer Matrices for Perfect Reconstruction Multirate Filter Bank Application", *IEEE Trans. on ASSP*, pp. 1561-1574, Oct. 1988.

[46] Vaidyanathan, P. P., Nguyen, T. Q., Doganata, Z. and Saramaki, T., "Improved technique for design of perfect reconstruction FIR QMF banks with lossless polyphase matrices", *IEEE Trans. on ASSP*, pp. 1042-1056, July 1989.

[47] R. A. Gopinath, J. E. Odegard, and C. S. Burrus, "Optimal wavelet representation of signals and the wavelet sampling theorem," *IEEE Trans. CAS II*, 41 (1994), pp. 262-277.

[48] Mallat, S., "A Theory for multiresolution signal decomposition: the wavelet representation," *IEEE Trans. PAMI*, vol. 11, pp. 674-693, 1989.

[49] Rioul, O., "A Discrete-time multiresolution theory," *IEEE Trans. on SP*, 41 (1993), pp. 2591-2606.

[50] Cohen, A., *Ondelettes, analyses multirésolutions et traitement numérique du signal,* Ph.D. thesis, Universite Paris IX, Dauphine, 1990.

[51] Lawton, W., "Necessary and sufficient conditions for construction orthonormal wavelet bases", *J. Math. Phys.,* 32 (1991), pp. 57-61.

[52] P. Steffen, P. N. Heller, R. A. Gopinath, C. S. Burrus, "Theory of Regular M-band Wavelets," *IEEE Trans. on SP,* 41 (1993), pp. 3497-3511.

[53] J. Princen and A. Bradley, "Analysis/Synthesis Filter Bank Design Based on Time Domain Aliasing Cancellation," *IEEE Trans. on ASSP*, pp. 1153-1161, Oct. 1986.

[54] Fliege, N., "Computational Efficiency of Modified DFT Polyphase Filter Banks," *Proc. of 27th asilomar Conference on Signals, Systems and Computers,* pp. 1296-1300, Nov. 1993.

[55] Lin, Y-P and Vaidyanthan, P. P., "Linear-phase Cosine-modulated Maximally-decimated filter banks with perfect reconstruction," *Proc. ISCAS,*, pp. 2.17 - 2.20.

[56] T. Q. Nguyen and R. D. Koilpillai, "The design of arbitrary-length cosine-modulated filter banks and wavelets, satisfying perfect reconstruction," *Proceeding of the IEEE-SP Int. Symp. on Time-Frequency and Time-Scale Analysis*, pp. 299-302, Victoria, Cananda, Oct. 1992.

[57] J. Mau, "Perfect-Reconstruction Modulated Filter Banks," *Proc. ICASSP*, 1992.

[58] Gopinath, R. and Burrus, C., "Theory of Modulated Filter Banks and Modulated Wavelet Tight Frames", *Proceeding of of ICASSP 93*, pp. III169-III172.

[59] T. Q. Nguyen, T. I. Laakso and T. E. Tuncer, "On Perfect-Reconstruction Allpass-Based Cosine-Modulated IIR Filter Banks", *Proceeding of ISCAS 94*, pp. 2-33 – 2-36.

[60] T. Q. Nguyen, "A class of generalized cosine-modulated filter bank," *Proc. ISCAS*, pp. 934-946, May 1992.

[61] Nayebi, K., Barnwell, T. P. III and Smith, M. J. T., "Low-delay FIR filter banks, design and evaluation", *IEEE Trans. on SP*, pp. 24-31, Jan. 94.

[62] Djohan, A., Nguyen, T. Q. and Tompkins, W. J., "ECG compression using discrete symmetric wavelet transform," *submitted to Int. Conf. IEEE EMBS*, 1995.